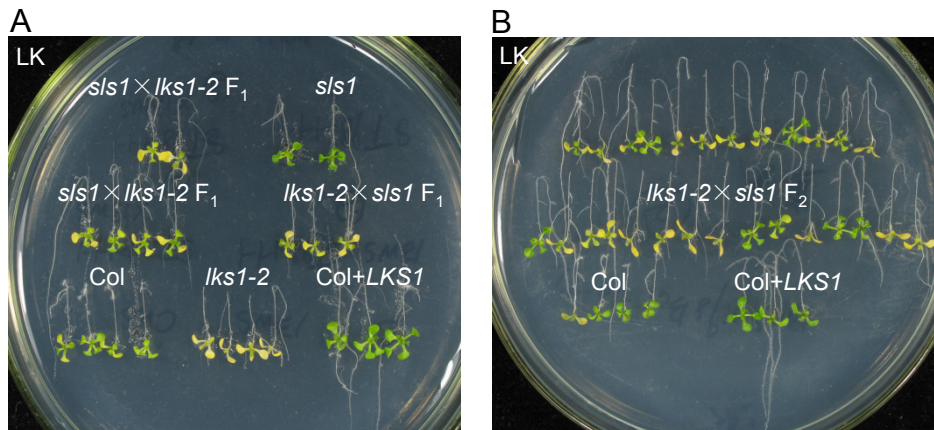


Supplemental Figure 1



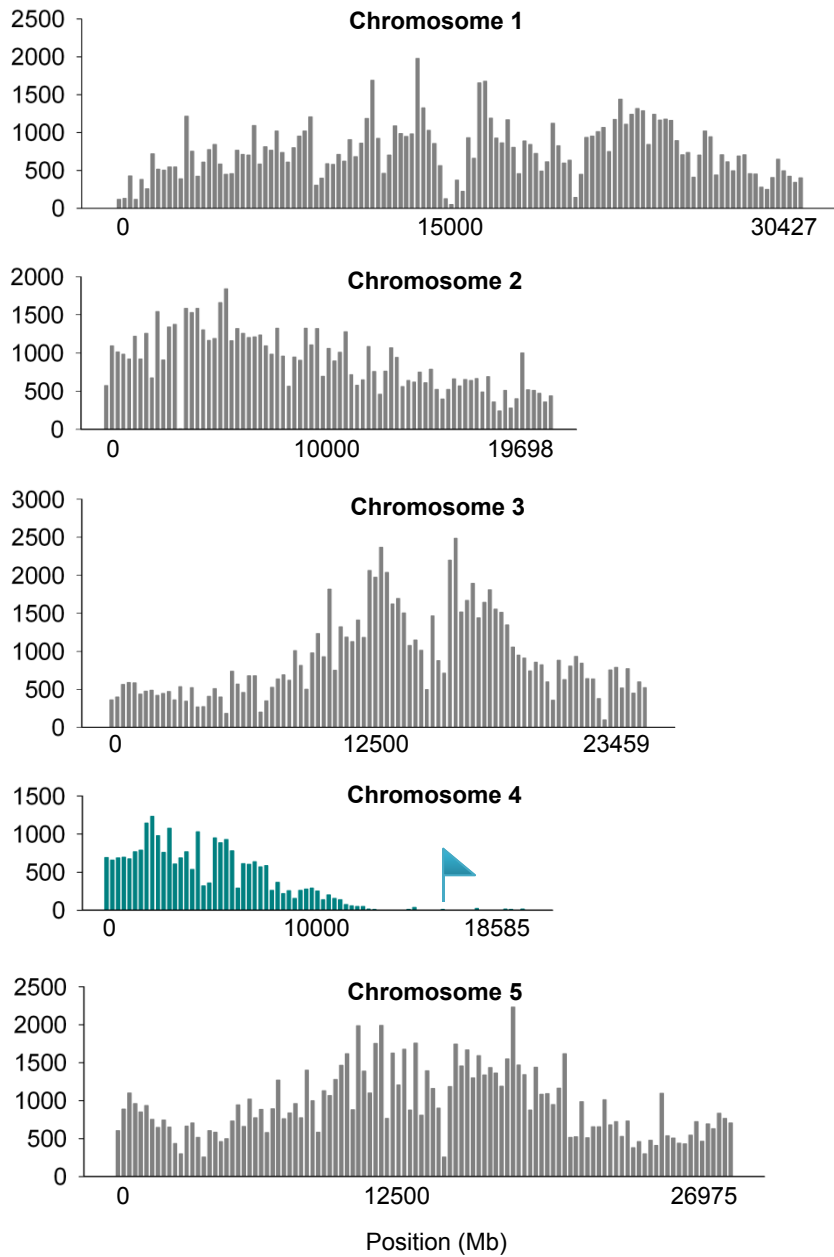
Supplemental Figure 1. Genetic analysis of *s/s1* mutant.

(A) and (B) Phenotype assay of F₁ (A) and F₂ (B) progenies of *s/s1* and *lks1-2* on LK medium. The photographs were taken 10 days after transferring from MS to LK medium. The table showed the phenotype segregation of F₂ progenies.

Genetic Analysis of *s/s1* Mutants.

| Cross (♀ × ♂) | Generation | Total seedlings tested | Low-K ⁺ sensitive | Low-K ⁺ insensitive | χ ² |
|-----------------------------|----------------|------------------------------|---------------------------------|-----------------------------------|----------------|
| <i>lks1-2</i> × <i>s/s1</i> | F ₂ | 782 | 589 | 193 | 0.00012 |

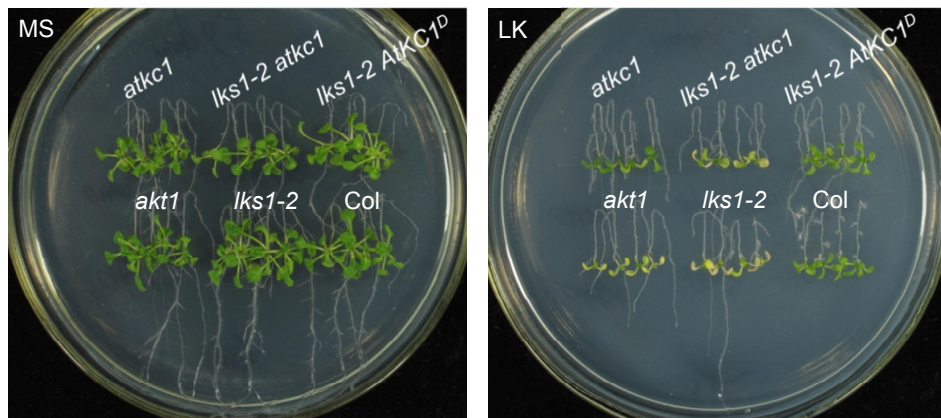
Supplemental Figure 2



Supplemental Figure 2. Genome-wide SNP analysis of *s/s1* mapping population using next generation mapping technique.

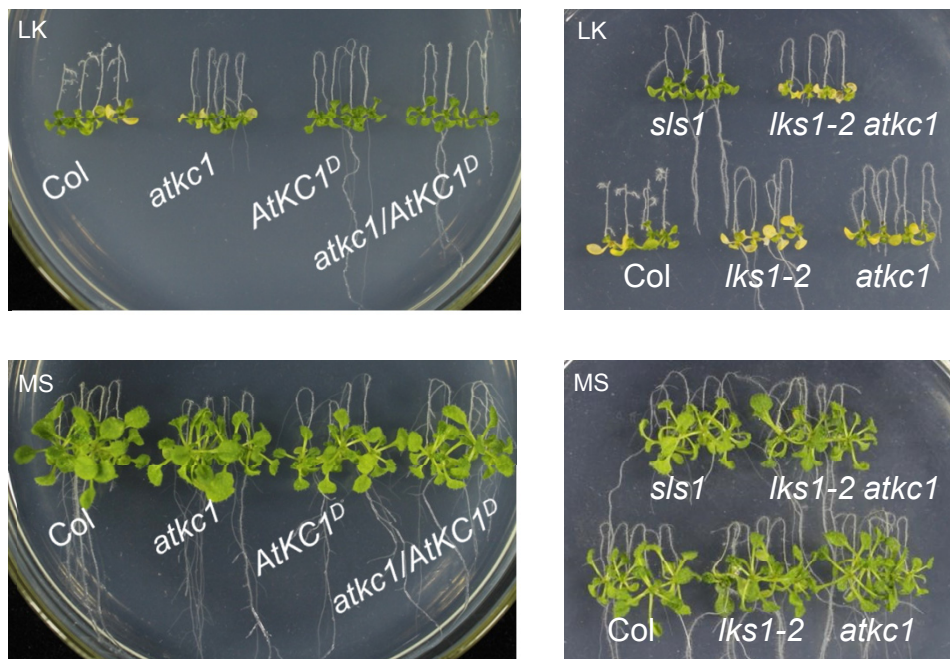
Genome-wide SNPs are shown by their chromosome positions. Filtered SNPs were collected over 250 kb intervals. There was non-recombinant block near the end of chromosome 4 (marked with a flag), which was consistent with the results from traditional map-based cloning.

Supplemental Figure 3



Supplemental Figure 3. The *atkc1* could not suppress the LK-sensitive phenotype of *lks1-2*. Phenotype comparison of the various mutant plants after grown on MS or LK medium for 10 days.

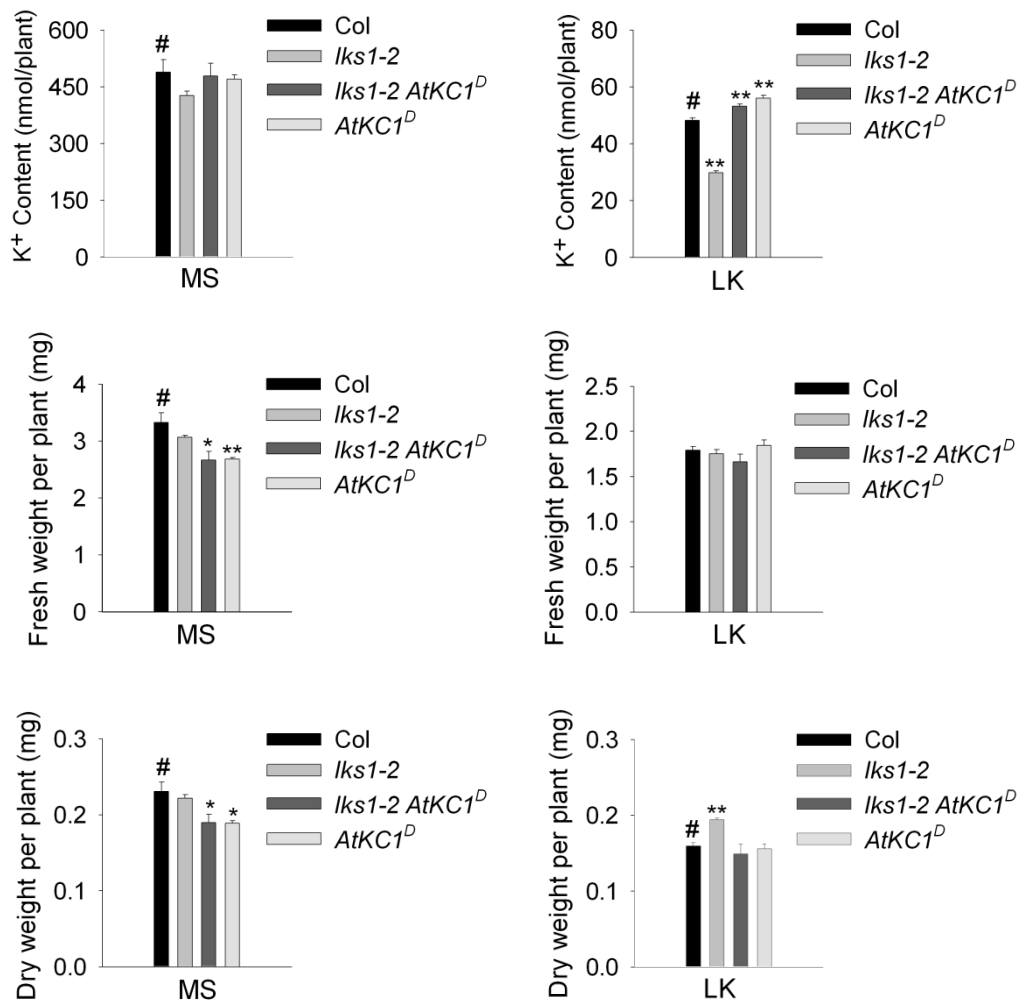
Supplemental Figure 4



Supplemental Figure 4. The *AtKC1^D* and *sis1* showed a LK-tolerant phenotype on LK medium.

Phenotype comparison of various mutant plants after growth on LK or MS medium for 12 days.

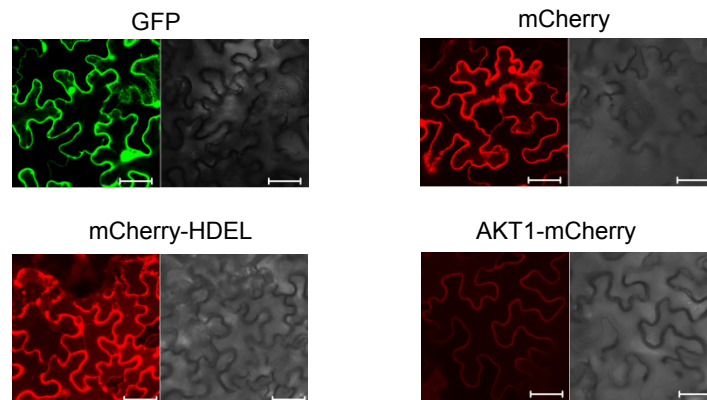
Supplemental Figure 5



Supplemental Figure 5. Total K⁺ content and biomass analyses of *lks1 AtKC1^D* and *AtKC1^D*.

The total K⁺ content and biomass were measured after the plants were transferred to MS or LK medium for 10 days. Data are shown as means \pm SE (n=4). The Student's *t* test (*P<0.05, **P<0.01) was used to determine the statistical significance.

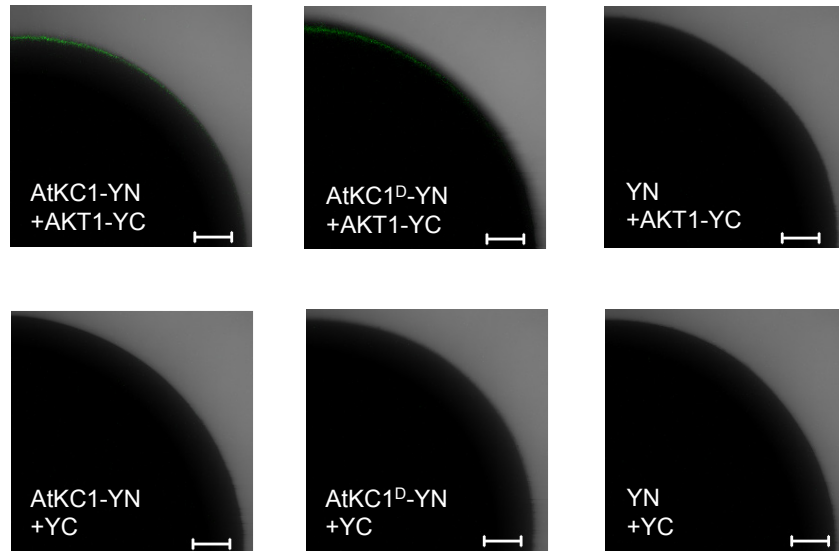
Supplemental Figure 6



Supplemental Figure 6. Subcellular localization of mCherry-HDEL and AKT1-mCherry in tobacco leaves.

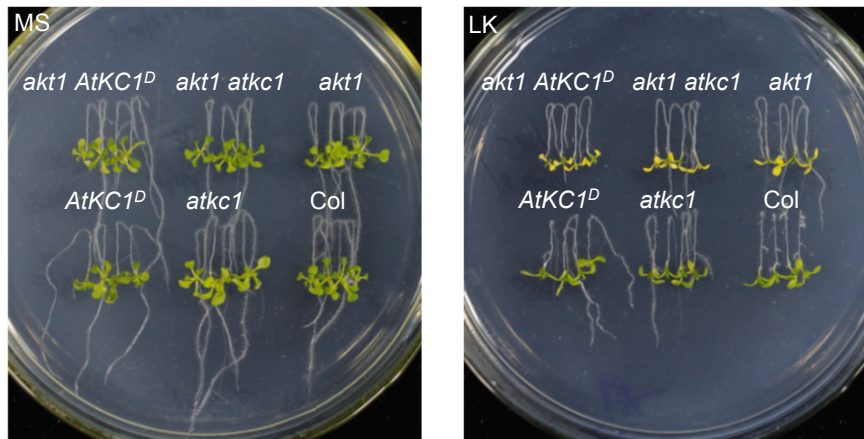
The mCherry-HDEL and AKT1-mCherry were located at the ER and PM respectively. GFP and mCherry showed nonspecific subcellular localization. Bars=50 μ m.

Supplemental Figure 7



Supplemental Figure 7. The protein interaction between AKT1 and AtKC1 or AtKC1^D in *Xenopus* oocytes using the BiFC method. Co-expression of AtKC1-YN or AtKC1^D-YN (YN, N-terminus of YFP) with AKT1-YC (YC, C-terminus of YFP) complemented YFP fluorescence at the plasma membrane. The point mutations in AtKC1^D did not affect its interaction with AKT1. Scale bars=100 μ m.

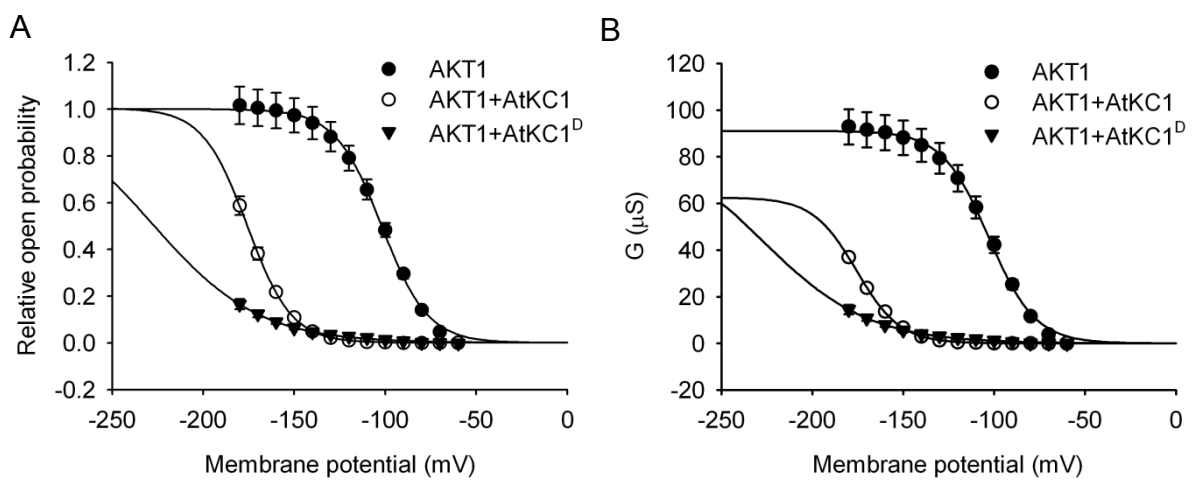
Supplemental Figure 8



Supplemental Figure 8. Neither *AtKC1^D* nor *atkc1* could suppress the LK-sensitive phenotype of *akt1*.

Phenotype comparison of various mutant plants after growth on MS or LK medium for 7 days.

Supplemental Figure 9



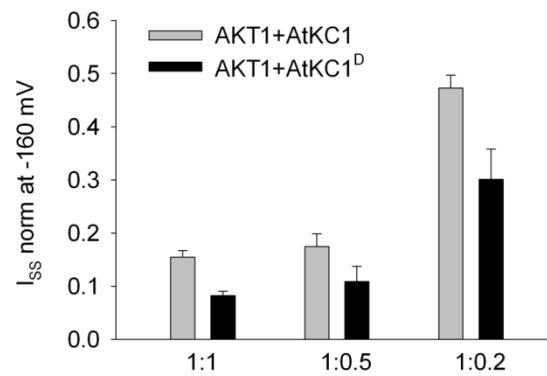
Supplemental Figure 9. The open probability and chord conductance analyses of AKT1 in *Xenopus* oocytes.

(A) The voltage dependence of inward K⁺ currents. The solid lines fits to the Boltzmann functions: relative open probability (G/G_{\max}) = $1/(1 + \exp((V_m - V_{1/2})/S))$.

Data are shown as means \pm SE (n=4).

(B) The G-V relationship of AKT1 steady-state currents in different combination. G (chord conductance) were calculated as $G=I/(V_m-E_K)$.

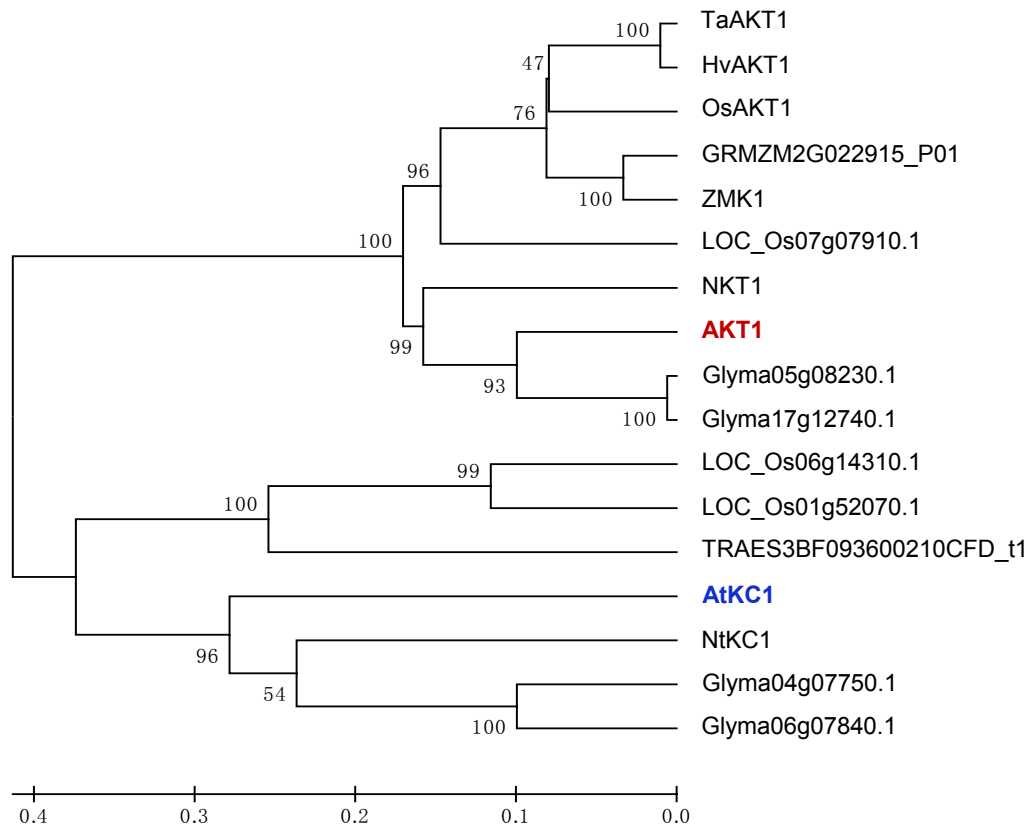
Supplemental Figure 10



Supplemental Figure 10. The dosage effect of AtKC1 or AtKC1^D on AKT1 activity.

Normalized AKT1 steady-state currents (I_{ss}) in oocytes injected with different ratios of AKT1:AtKC1 or AtKC1^D at -160 mV. The currents under different ratio were normalized to the currents value of AKT1, respectively. CIPK23 and CBL1 are included in all combinations. Data are shown as means \pm SE ($n \geq 4$).

Supplemental Figure 11



Supplemental Figure 11. Phylogenetic analysis of AKT1 and AtKC1 homologs in different crops.

The sequences were aligned in ClustalX2 program, and the phylogenetic tree was constructed using MEGA Software. The phylogenetic analysis included 17 sequences from seven plant species, including *Arabidopsis thaliana*, *Nicotiana tabacum*, *Glycine max*, *Oryza sativa*, *Zea mays*, *Triticum aestivum*, and *Hordeum vulgare*. The sequence information was collected from the following websites:

Nicotiana tabacum (<http://www.ebi.ac.uk/>) AB196790 (NKT1), AB196791 (NtKC1);

Glycine max (<http://www.plantgdb.org/GmGDB/>) Glyma05g08230.1, Glyma17g12740.1, Glyma04g07750.1, Glyma06g07840.1;

Oryza sativa (<http://rice.plantbiology.msu.edu/>) LOC_Os01g45990.1 (OsAKT1), LOC_Os07g07910.1, LOC_Os06g14310.1, LOC_Os01g52070.1;

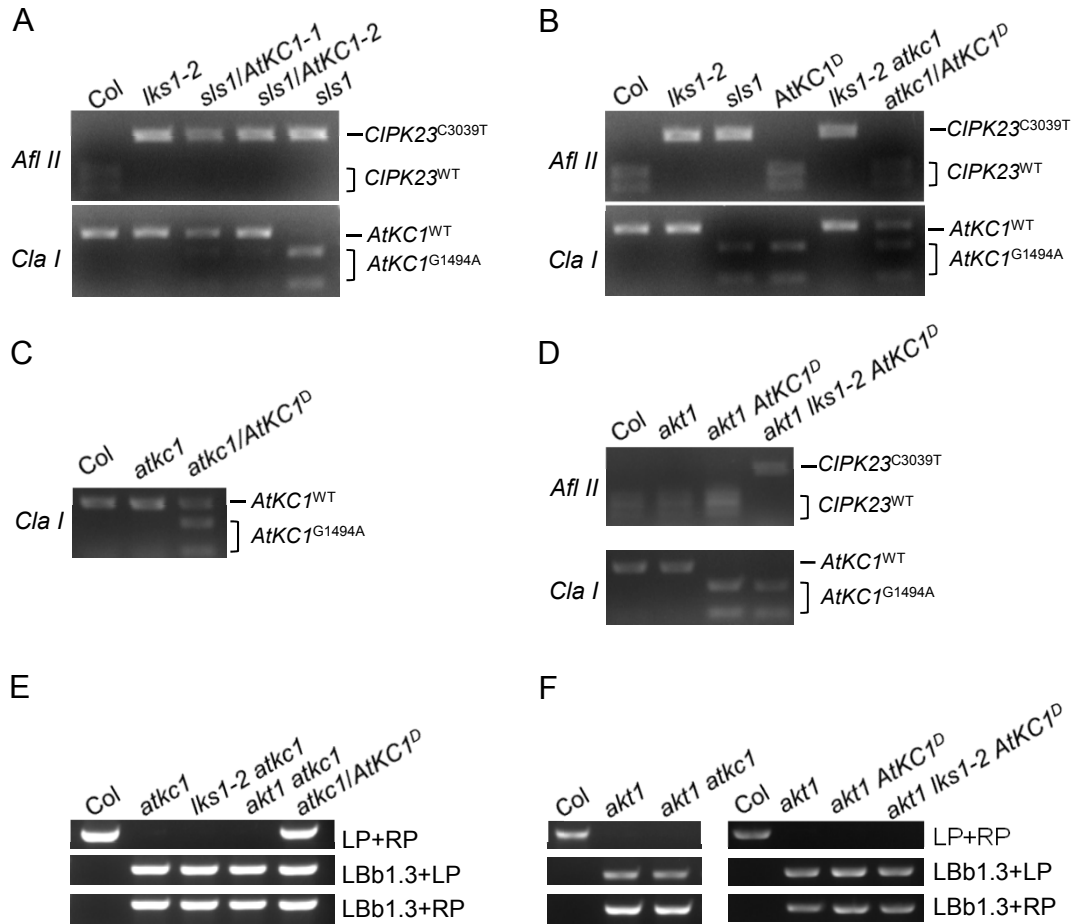
Zea mays (<http://plants.ensembl.org/index.html>) GRMZM2G171279_P01 (ZMK1), GRMZM2G022915_P01;

Triticum aestivum (<http://plants.ensembl.org/index.html>)

TRAES3BF087600020CFD_t1/Traes_3B_1795B9E0B.1 (TaAKT1), TRAES3BF093600210CFD_t1;

Hordeum vulgare (<http://plants.ensembl.org/index.html>) MLOC_74879.2 (HvAKT1).

Supplemental Figure 12



Supplemental Figure 12. Molecular verification of various plant materials.

(A) to (D) The genotypes of *CIPK23* and *AtKC1* in different plant materials were confirmed using cleaved amplified polymorphic sequences (CAPS) markers. The restriction enzymes *Afl II* and *Cla I* were used to identify wild-type and mutant forms of *CIPK23* and *AtKC1*, respectively.

(E) T-DNA insertion verification of *atkc1* (SALK_140579).

(F) T-DNA insertion verification of *akt1* (SALK_071803).

Supplemental Table 1

Supplemental Table 1. The primer sequences used in this study.

| Gene | Primer Name | Primer Sequence (5'-3') | Assay or Vector Design |
|--------------------------------------|--------------|---|---------------------------------------|
| For Genotyping | | | |
| CIPK23 | C3039T-F | TGGAGTTGTGTATTGGTTTGTG | CAPS |
| | C3039T-R | TCTGCTCCACTTCTTGACGC | |
| AtKC1 | G1494A-F | GCACATTCAACTATTTTCG | CAPS |
| | G1494A-R | TTCTTGCTTGTGTATCGC | |
| AtKC1 | AtKC1-LP | AACCAACATCTATTCCGCTCC | T-DNA |
| | AtKC1-RP | TCCTCATCGTTACTTTGTGGTG | |
| AKT1 | AKT1-LP | TCCATGTCAAAGCTAAGAAGACG | T-DNA |
| | AKT1-RP | TCGGTGATAGATAGTGGTGCC | |
| For Real-time PCR | | | |
| AtKC1 | KC1-F | ATTGCTTCCAAGGGTGTGAG | Q-PCR |
| | KC1-R | GCGTGCACGTCATTATCAGA | |
| ACTIN2/8 | ACTIN2/8-F | ACGGTAACATTGTGCTCAGTGGTG | Q-PCR |
| | ACTIN2/8-R | CTTGGAGATCCACATCTGCTGGA | |
| For Cloning | | | |
| AtKC1 | AtKC1pg-F | <u>GGGGTACCT</u> GCCAAACAAAACAAAGAG | pCAMBIA1300 |
| | AtKC1pg-R | CGGGATCCTAGGAGTCCTTACAGAAAGTTTC | |
| AtKC1 | AtKC1c-F | <u>CGGATCC</u> ATGTCTACGACGACTAC | SUPERR:sXVE:GFP _c :Bar |
| | AtKC1c-R | <u>GGGTACC</u> GAAAATATATAAATGATCG | |
| AKT1 | AKT1c-F | <u>GCTCTAGA</u> ATGAGAGGAGGGGCTTTG | SUPERR:sXVE:mCherry _c :Bar |
| | AKT1c-R | TCCCCCGGGAGAATCAGTTGCAAAGATG | |
| AtKC1 | AtKC1c2-F | TTTT <u>ACTAGT</u> ATGTCTACGACGACTACTGAGG | pGEMKN-YN-MCS |
| | AtKC1c2-R | TTTT <u>GCGGCCG</u> CTTAGAAAATATATAAATGATCG | |
| AKT1 | AKT1c2-F | CACCCCCGGGATGAGAGGAGGGGCTTTG | pGEMKN-MCS-YC |
| | AKT1c2-R | CGGAATTCAGAATCAGTTGCAAAGATG | |
| For Site-Directed Mutagenesis | | | |
| AtKC1 | KC1 G1494A-F | GCCTCACTTCTTATATCATCGATATCATGACCAAT | pCAMBIA1300 |
| | | CTAGTTGT | |
| | KC1 G1494A-R | ACAACTAGATTGGTCATGATATCGATGATATAAG | |
| | | AAGTGAGGC | |